

PREPARATION AND PHOTOELECTROCHEMICAL PROPERTIES OF TiO₂ NANOTUBE AND TiO₂ NANOWIRES ARRAYS

TỔNG HỢP VÀ NGHIÊN CỨU NHỮNG TÍNH CHẤT QUANG ĐIỆN HÓA CỦA VẬT LIỆU NANO TiO₂ MẢNG ỐNG VÀ MẢNG SỢI

Nguyễn Văn Mạnh^{1,*},
Nguyễn Quang Tùng¹, Bùi Sơn Hải²

ABSTRACT

In this paper, synthesis, nanostructures, characterization, and photoelectrochemical (PEC) properties of TiO₂ nanotube arrays (NTA) and TiO₂ nano wires (NWs) are described in detail. The information of charges transporting of nanotube arrays (NTA) and nanowires (NWs) have been discussed in this paper. The electron/hole recombination in the NTA and NWs are also compared.

Keywords: TiO₂ nano, nanostructure, photoelectrochemical.

TÓM TẮT

Trong bài báo này, phương pháp tổng hợp, cấu trúc vật liệu, các đặc trưng và tính chất quang điện hóa (PEC) của mảng ống nano TiO₂ (NTA) và mảng sợi nano TiO₂ (NWs) được mô tả chi tiết. Những thông tin về sự chuyển điện tích trong mảng ống nano (NTA) và mảng sợi nano (NWs) đã được thảo luận trong bài báo này. Sự tái tổ hợp các điện tích - lỗ hổng trong NTA và NWs cũng được đưa ra so sánh.

Từ khóa: Nano TiO₂, cấu trúc nano, tính chất quang điện hóa.

¹Khoa Công nghệ Hóa, Trường Đại học Công nghiệp Hà Nội

²Trung tâm Cơ khí, Trường Đại học Công nghiệp Hà Nội

*Email: manhtb0919@gmail.com

Ngày nhận bài: 17/01/2018

Ngày nhận bài sửa sau phản biện: 28/03/2018

Ngày chấp nhận đăng: 25/04/2018

1. INTRODUCTION

Since Fujishima and Honda discovered the photocatalytic splitting of water on TiO₂ semiconductor in 1972 [1], thenceforth TiO₂ photocatalyst is becoming increasingly attractive for potential and versatile applications in energy and environment fields. In comparison with other semiconductors, TiO₂ has attracted great interest due to its advantages as chemical inertness [2], non-toxicity [3], low-cost [4], long-term stability against photocorrosion and chemical corrosion [5]. One-dimensional (1-D) nanostructured TiO₂, such as nanorod, nanowire, and nanotube have received significant attention due to its light confinement, efficient charge

separation, and high carrier mobility properties, all of which are beneficial for PEC performance enhancement [6-9].

The TiO₂ NTA has showed highly ordered vertically aligned tubular structure and large surface-to-volume ratio [10]. Several methods have been used to fabricate TiO₂ NTA such as deposition into a nanoporous alumina template, sol-gel transcription using organo-gelators as templates [11], seeded growth and anodization of titanium [12]. Among them anodization of titanium in electrolyte is most interesting for its optical and electric properties and surface area due highly ordered nanotube arrays with controllable dimensions [13-15]. Meanwhile, the TiO₂ NWs are one dimensional nanostructured, that is also considered for photovoltaic, energy conversion and photocatalytic applications due to its large surface-to-volume ratio allows for distinct structural and chemical behavior as well as greater chemical reactivity [7, 16, 17]. TiO₂ NWs can be fabricated by hydrothermal [18], chemical vapor deposition [19], pulse laser deposition [20].

In this work, highly ordered TiO₂ NTA and TiO₂ NWs are fabricated by anodization of titanium in NaF and NaHSO₄ based baths [21] and hydrothermal method [22], respectively. Herein, the samples were characterized by XRD, SEM, UV-vis and PL spectroscopy and photoelectrochemical properties are shown in detail.

2. EXPERIMENTAL PROCEDURES

2.1. Materials

Titanium foil (99.8% purity, 0.127 mm thick) was purchased from Aldrich (Milwaukee, WI). NaF, NaHSO₄, Na₂S (99.9%), Na₂SO₃ (99%), HCl, NaOH, acetone, methanol were obtained from Shanghai Chemical Corporation of China. All other reagents of analytical grade were obtained from commercial sources and used as received. Twice distilled water was used throughout the experiments.

2.2. Methods

2.1.1. Fabrication of TiO₂ nanotube array

Highly ordered TiO₂ NTA were prepared by anodic oxidation method in a two-electrode electrochemical cell. A 0.25 mm-thick titanium foil with a size of 1 cm × 4 cm

(99.7%, Adrich) was used as a working electrode, and a platinum foil served as a counter electrode. Titanium ribbons were cleaned in 3% hydrofluoric acid (30 seconds), twice distilled water, then ultrasonic cleaned for 10 min in acetone solution and ethanol. The cleaned titanium ribbon was anodized at 20 V in an electrolyte containing 0.1 M NaF and 0.5 M NaHSO₄ at room temperature for 2 hours in a two-electrode configuration with a platinum cathode [23]. The TiO₂ NTA samples were ultrasonic cleaned for 10 min in iso-propanol solution to remove the debris on the surface of nanotube arrays, dried in air, then annealed at 500°C for 3 hours in air with heating and cooling rate of 2°C min⁻¹.

2.1.2. Fabrication of TiO₂ nanowires

TiO₂ NWs was prepared by hydrothermal method [22, 24]. Titanium foil (3cm × 4cm) were cleaned in 3% hydrofluoric acid (30 seconds), twice distilled water, in acetone and ethanol ultrasonic cleaning each 5min, then ultrapure water repeatedly washed several times, dried by nitrogen and set aside. A 50ml of 4M NaOH aqueous solution were poured into Teflon-lined autoclave (inner liner volume 100mL). After put teflon-lined autoclave into an oil bath heated to a 220°C temperature, after 6 hours reaction at 220°C, the reactor was allowed to cool to room temperature. Remove the sample vessel open, soaking 60 mins by 0.5M HCl aqueous solution, then soaking and then ultrapure water several times. As-prepared sample dried in air, then annealed at 500°C for 3 hours in air with heating and cooling rate of 2°C min⁻¹. The film morphology evolution, crystal structure transformations and growth mechanism are described in detail [25, 26] by three-step process. First, the titanium foil reacts with NaOH to form Na₂Ti₂O₄(OH)₂ sheets, which exfoliate and spiral into nanotubes. Next, the Na₂Ti₂O₄(OH)₂ nanotubes were converted to H₂Ti₂O₄(OH)₂ nanotubes by Na₂Ti₂O₄(OH)₂ nanotubes immersed in HCl solution to replace the Na⁺ ions with H⁺ ions. Finally, the H₂Ti₂O₄(OH)₂ nanotubes were converted to polycrystalline anatase nanowires through a topotactic transformation by calcination.

2.2. Characterization

All electrochemical measurements were performed with a CHI electrochemical analyzer (CHI660B, Shanghai Chenhua Instrument Co. Ltd.) using a conventional three electrode system including a Ag/AgCl reference electrode, a Pt sheet counter electrode, and the as-prepared TiO₂ NTA/NWs as working electrode. The morphologies of the as-prepared materials were studied using scanning electron microscope (SEM, Hitachi S-4800). The crystalline phases of the samples was characterized by an X-ray diffractometer (XRD, M21X, MAC Science Ltd., Japan) with Cu Kα irradiation source and a scanning speed of 2°/min in the 2θ range of 20–80°. A 500 W Xe lamp (CHF-XQ-500 W, Beijing Changtuo Co., Ltd.) was used as the light source, filtered to 100 mW cm⁻² AM1.5G as determined by a radiometer (NOVA Oriel 70260). Photoelectrochemical properties were measured in 0.24 M Na₂S and 0.35M Na₂SO₃ aqueous solution. The fluorescence

spectra were taken with a fluorescence spectrophotometer (Hitachi F-4600). UV–vis absorption spectra of TiO₂ NTA, TiO₂ NWs photoelectrodes were recorded in the range from 200 to 800 nm using a UV–Visible Cary 300 spectrophotometer equipped with an integrating sphere of 150 mm in diameter.

3. RESULTS AND DISCUSSIONS

3.1. Characterization of the TiO₂ NTA and TiO₂ NWs

The surface morphologies of TiO₂ NTA obtained by SEM shown in figure 1 (A). TiO₂ NTA have an inner pore diameter ranging from 70 to 110 nm and an average length of 400 nm and wall thickness of about 17nm. The results have shown that the formation mechanism of the TiO₂ NTA is as well as previous reported [23, 27–29]. Figure 1 (B) shows the XRD spectrum of the TiO₂ phases before and after annealing at 500°C in air atmosphere. The annealed TiO₂ NTA film is appeared new two peaks at 2θ = 25.3° and 27.54°. This two peaks are anatase TiO₂ (101) (JCPDS No. 21-1272) and rutile TiO₂ (110) (JCPDS No. 04-0551), respectively. Beside, the peaks at 2θ = 38.56°, 40.3°, 53.1°, 63.06°, 70.76° representative of amorphous phase, which are indexed to the metal titanium phase (JCPDS No. 44-1294) [30].

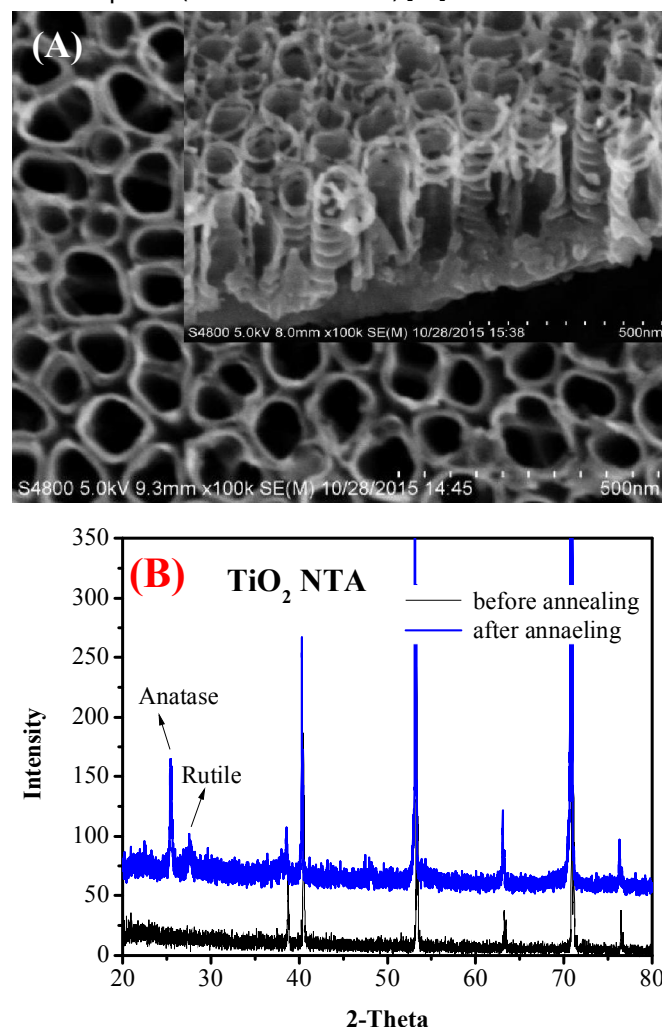


Figure 1. (A) Top-surface and cross insert section SEM image of TiO₂NTA, (B) XRD spectrum of TiO₂ NTA before and after annealing.

Figure 2 (A) shows the top-view SEM image and cross insert sectional SEM image of TiO₂ NWs. As shown in figure 2 (A), the TiO₂ NWs with thickness in the range of 25–100 nm, (see on the left of insert image) and an average length about 5 μm (see on the right of insert image). The results have shown that the formation mechanism of the TiO₂ NWs is well documented [18, 24, 31]. As shown in Figure 2 (B), the unannealed TiO₂ NWs have a pick at 2θ = 24.56°, which relies on the anatase protonated bititanate H₂Ti₂O₄(OH)₂ nanowires phase. The annealed sample shows the two picks at 2θ values of 25.39° and 27.5°, which are anatase TiO₂ (101) (JCPDS No. 21-1272) and rutile TiO₂ (110) (JCPDS No. 04-0551), respectively. The other peaks at 2θ values of 37.8°, 38.5°, 48.0°, 53.89°, 55.0°, 62.9°, 68.8°, 70.3°, 75.0° can be well-indexed to (004), (112), (200), (105), (211), (204), (116), (200) and (215) crystal planes of anatase TiO₂(JCPDS No. 21–1272), respectively, which shows that the protonated bititanate H₂Ti₂O₄(OH)₂ nanowires is converted to single crystalline anatase TiO₂ nanowires through a topotactic transformation by calcination.

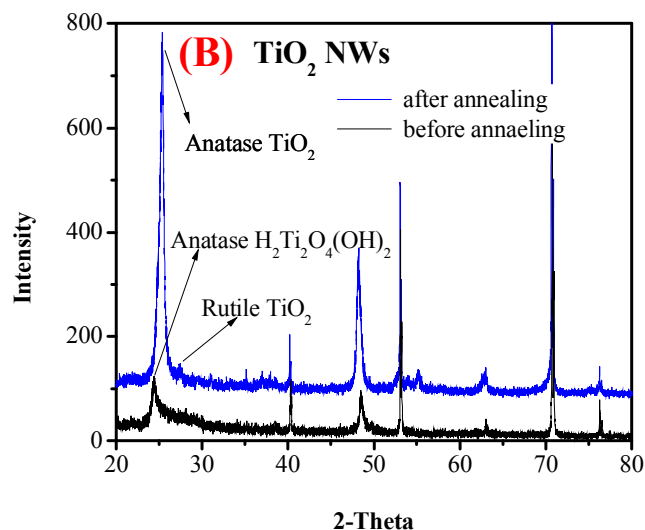
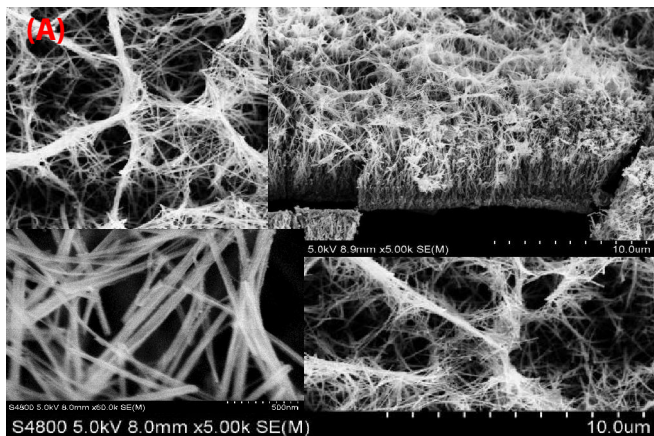


Figure 2. (A) Top-surface and cross insert section SEM image of TiO₂NWs, left insert is the FESEM image of TiO₂NWs (B) XRD spectrum of TiO₂ NWs before and after annealing

Figure 3 shows the photoluminescence (PL) emission spectrum of TiO₂ NTA and TiO₂ NWs with the excitation

wavelength at 270 nm. PL spectrum has been widely used to investigate the efficiency of charge carrier trapping, immigration, and transfer, and to understand the fate of electron/hole pairs in semiconductor particles. Charge carriers are trapped at the defects of semiconductors which have different energy levels and trapping events might reduce chances for electron-hole recombination and increase electron lifetime[32-34]. As shown in figure 3, the lower peak intensities of TiO₂ NTA revealed the recombination rate of photogenerated charges on the TiO₂ NTA surface are slower than on the TiO₂ NWs surface. These maybe related to the prepared samples, which is different in the phase structure and morphologies. These differences can be explained by a different degree of formed oxygen vacancies due to different experimental conditions (temperature, aging time) during synthesis [32].

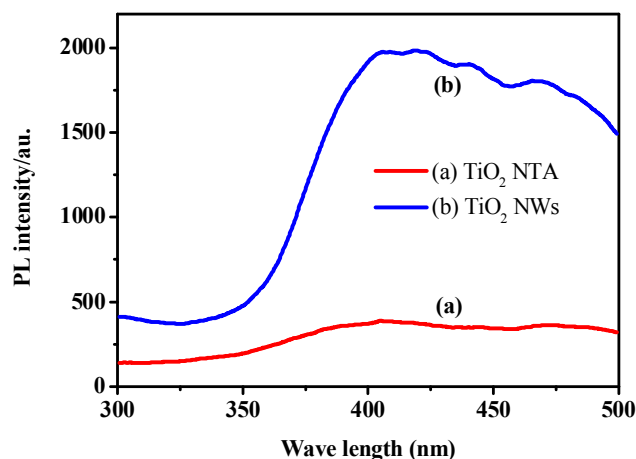


Figure 3. Emission spectra of (a) TiO₂NTA and (b) TiO₂NWs. Emission spectra were recorded with 270 nm excitation.

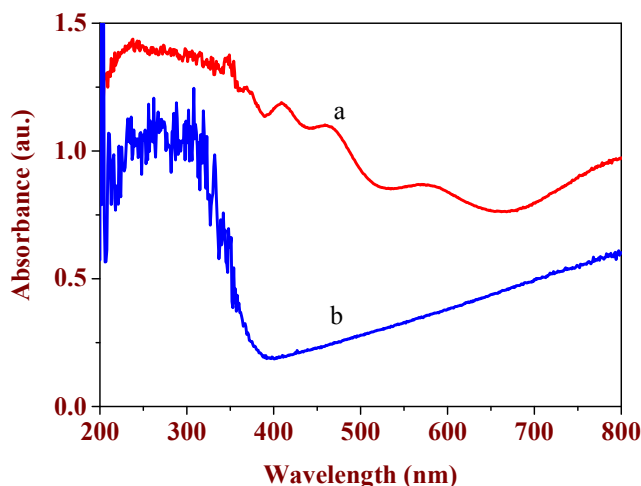


Figure 4. UV-Vis spectra of TiO₂ nanotube array (a) and TiO₂ nanowires (b)

The UV-Vis diffuse reflectance absorbance spectra of the TiO₂ NTA and TiO₂ NWs are exhibited in Figure 4. As shown in figure 4 (a), the characteristic absorption peaks of TiO₂ NTA at 390 nm due to the result from the absorption of the trapped holes, the other two picks at 475 nm and 585 nm, which result from the absorption of the trapped electrons

[35]. Meanwhile, TiO₂ NWs is only absorptive in UV light region as shown in figure 4(a). Clear differences of PL and absorption properties depending on process of synthesis the samples.

3.2. Photoelectrochemical properties of the TiO₂ NTA and TiO₂ NWs

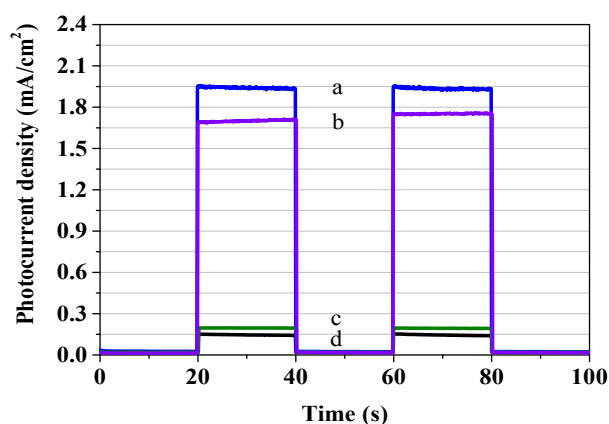


Figure 5. Photocurrent response of TiO₂ nanotube arrays (a, c) and TiO₂ nanowires (b, d). Herein (a, b) are measured in 0.24M Na₂S and 0.35M Na₂SO₃ solution, (c, d) are measured in 0.05M Na₂SO₄ solution

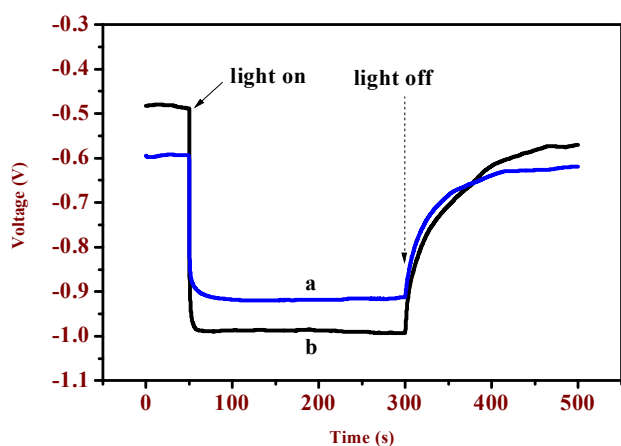


Figure 6. Open-circuit photovoltage response of (a) TiO₂NTA and (b) TiO₂NWs measured in 0.24M Na₂S and 0.35M Na₂SO₃ solution

Figure 5 shows the photocurrent density response of TiO₂ NTA and TiO₂ NWs are measured in different electrolytes. Figure 5 indicated that the photocurrent response of TiO₂ NTA of both the 0.24M Na₂S and 0.35M Na₂SO₃ solution and 0.05M Na₂SO₄ solution is higher than TiO₂ NWs. The photocurrent density of TiO₂ NTA and TiO₂ NWs measured in 0.24M Na₂S and 0.35M Na₂SO₃ solution are 1.95 mA cm⁻² and a 1.7 mA cm⁻², respectively, while in 0.05M Na₂SO₄ solution are only 0.2 mA cm⁻² and a 0.15 mA cm⁻², respectively. Photocurrent response of both TiO₂ NTA and TiO₂ NWs measured in 0.24M Na₂S and 0.35M Na₂SO₃ solution are higher than in 0.05M Na₂SO₄ solution. These results implicated that under illumination the free photogenerated electrons/holes from TiO₂ NTA electrode are more than TiO₂ NWs. Figure 6 shows the open-circuit photovoltage response of (a) TiO₂ NTA and (b) TiO₂ NWs

measured in 0.24M Na₂S and 0.35M Na₂SO₃ solution. Under illumination electrons and holes are generated. When the illumination is stopped, the free electrons are slowly recombination with holes trapped in the TiO₂ and dissolved oxygen in the electrolyte, which scavenges electrons. The electron recombination rate relates with the electron lifetime (τ_n). It is determined by following equation 1 [15].

$$\tau_n = [-k_B T / e] [dV_{oc} / dt]^{-1} \quad (1)$$

Where $k_B T$ is the thermal energy, e is the positive elementary charge, and dV_{oc} / dt is the open-circuit voltage transient. (Eq. 1) shows that the τ_n increasing with increasing value of the $[dV_{oc} / dt]$. As shown in figure 6, the V_{oc} of TiO₂ NTA higher value than TiO₂ NWs. The longer lifetimes seen in the nanotube array films indicate relatively fewer recombination centers.

4. SUMMARY

The TiO₂ NTA has been obtained through titanium anodization in NaF and NaHSO₄ solution. The TiO₂ NWs have also been fabricated by hydrothermal method. The resulting characterization and photoelectrochemical properties showed that the highly ordered and vertically aligned TiO₂ NTA is better than TiO₂ NWs. As prepared, TiO₂ NTA will be used in the following photoelectrochemical applications.

TÀI LIỆU THAM KHẢO

- [1]. Fujishima A, Honda K, 1972. *Electrochemical Photolysis of Water at a Semiconductor Electrode*. Nature, 238(5358): 37-38.
- [2]. Huang Q, Tian S, Zeng D, et al, 2013. *Enhanced Photocatalytic Activity of Chemically Bonded TiO₂/Graphene Composites Based on the Effective Interfacial Charge Transfer through the C-Ti Bond*. ACS Catalysis, 3(7): 1477-1485.
- [3]. Albu S P, Ghicov A, Macak J M, et al, 2007. *Self-Organized, Free-Standing TiO₂ Nanotube Membrane for Flow-through Photocatalytic Applications*. Nano Letters, 7(5): 1286-1289.
- [4]. Xu Z, Huang C, Wang L, et al, 2015. *Sulfate Functionalized Fe₂O₃ Nanoparticles on TiO₂ Nanotube as Efficient Visible Light-Active Photo-Fenton Catalyst*. Industrial & Engineering Chemistry Research, 54(16): 4593-4602.
- [5]. Wang H, Zhu W, Chong B, et al, 2014. *Improvement of photocatalytic hydrogen generation from CdSe/CdS/TiO₂ nanotube-array coaxial heterogeneous structure*. International Journal of Hydrogen Energy, 39(1): 90-99.
- [6]. Hwang Y J, Yang S, Jeon E H, et al, 2016. *Photocatalytic oxidation activities of TiO₂ nanorod arrays: A surface spectroscopic analysis*. Applied Catalysis B: Environmental, 180(480-486).
- [7]. Györi Z, Kónya Z, Kukovec Á, 2015. *Visible light activation photocatalytic performance of PbSe quantum dot sensitized TiO₂ Nanowires*. Applied Catalysis B: Environmental, 179(583-588).
- [8]. Horváth E, Kukovec Á, Kónya Z, et al, 2007. *Hydrothermal Conversion of Self-Assembled Titanate Nanotubes into Nanowires in a Revolving Autoclave*. Chemistry of Materials, 19(4): 927-931.
- [9]. Razzaq A, Grimes C A, In S-I, 2016. *Facile fabrication of a noble metal-free photocatalyst: TiO₂ nanotube arrays covered with reduced graphene oxide*. Carbon, 98(537-544).

- [10]. Varghese O K, Paulose M, LaTempa T J, et al, 2009. *High-Rate Solar Photocatalytic Conversion of CO₂ and Water Vapor to Hydrocarbon Fuels*. *Nano Letters*, 9(2): 731-737.
- [11]. Lakshmi B B, Dorhout P K, Martin C R, 1997. *Sol-Gel Template Synthesis of Semiconductor Nanostructures*. *Chemistry of Materials*, 9(3): 857-862.
- [12]. Chen X, Mao S S, 2007. *Titanium Dioxide Nanomaterials: Synthesis, Properties, Modifications, and Applications*. *Chemical Reviews*, 107(7): 2891-2959.
- [13]. Allam N K, Grimes C A, 2008. *Effect of cathode material on the morphology and photoelectrochemical properties of vertically oriented TiO₂ nanotube arrays*. *Solar Energy Materials and Solar Cells*, 92(11): 1468-1475.
- [14]. Cao G, Liu D, 2008. *Template-based synthesis of nanorod, nanowire, and nanotube arrays*. *Advances in Colloid and Interface Science*, 136(1-2): 45-64.
- [15]. Mor G K, Varghese O K, Paulose M, et al, 2006. *A review on highly ordered, vertically oriented TiO₂ nanotube arrays: Fabrication, material properties, and solar energy applications*. *Solar Energy Materials and Solar Cells*, 90(14): 2011-2075.
- [16]. Shankar K, Basham J I, Allam N K, et al, 2009. *Recent Advances in the Use of TiO₂ Nanotube and Nanowire Arrays for Oxidative Photoelectrochemistry*. *The Journal of Physical Chemistry C*, 113(16): 6327-6359.
- [17]. Hochbaum A I, Yang P, 2010. *Semiconductor Nanowires for Energy Conversion*. *Chemical Reviews*, 110(1): 527-546.
- [18]. Liu C, Zhang L, Liu R, et al, 2016. *Hydrothermal synthesis of N-doped TiO₂ nanowires and N-doped graphene heterostructures with enhanced photocatalytic properties*. *Journal of Alloys and Compounds*, 656: 24-32.
- [19]. Du J, Gu X, Guo H, et al, 2015. *Self-induced preparation of TiO₂ nanowires by chemical vapor deposition*. *Journal of Crystal Growth*, 427:54-59.
- [20]. Nechache R, Nicklaus M, Diffalah N, et al, 2014. *Pulsed laser deposition growth of rutile TiO₂ nanowires on Silicon substrates*. *Applied Surface Science*, 313(48-52).
- [21]. Gong D, Grimes C A, Varghese O K, et al, 2001. *Titanium oxide nanotube arrays prepared by anodic oxidation*. *Journal of Materials Research*, 16(12): 3331-3334.
- [22]. Arcadipane E, Sanz R, Miritello M, et al, 2016. *TiO₂ nanowires on Ti thin film for water purification*. *Materials Science in Semiconductor Processing*, 42, Part : 24-27.
- [23]. Yang L, Yang W, Cai Q, 2007. *Well-Dispersed PtAu Nanoparticles Loaded into Anodic Titania Nanotubes: A High Antipoison and Stable Catalyst System for Methanol Oxidation in Alkaline Media*. *The Journal of Physical Chemistry C*, 111(44): 16613-16617.
- [24]. Tahir M, Tahir B, Amin N A S, 2015. *Gold-nanoparticle-modified TiO₂ nanowires for plasmon-enhanced photocatalytic CO₂ reduction with H₂ under visible light irradiation*. *Applied Surface Science*, 356: 1289-1299.
- [25]. Boercker J E, Enache-Pommer E, Aydil E S, 2008. *Growth mechanism of titanium dioxide nanowires for dye-sensitized solar cells*. *Nanotechnology*, 19(9): 095604.
- [26]. Liu B, Boercker J E, Aydil E S, 2008. *Oriented single crystalline titanium dioxide nanowires*. *Nanotechnology*, 19(50): 505604.
- [27]. Liu Z, Zhang X, Nishimoto S, et al, 2008. *Highly Ordered TiO₂ Nanotube Arrays with Controllable Length for Photoelectrocatalytic Degradation of Phenol*. *The Journal of Physical Chemistry C*, 112(1): 253-259.
- [28]. Kang Q, Lu Q Z, Liu S H, et al, 2010. *A ternary hybrid CdS/Pt-TiO₂ nanotube structure for photoelectrocatalytic bactericidal effects on Escherichia Coli*. *Biomaterials*, 31(12): 3317-3326.
- [29]. Kang Q, Liu S, Yang L, et al, 2011. *Fabrication of PbS Nanoparticle-Sensitized TiO₂ Nanotube Arrays and Their Photoelectrochemical Properties*. *ACS Applied Materials & Interfaces*, 3(3): 746-749.
- [30]. Yu J, Dai G, Cheng B, 2010. *Effect of Crystallization Methods on Morphology and Photocatalytic Activity of Anodized TiO₂ Nanotube Array Films*. *The Journal of Physical Chemistry C*, 114(45): 19378-19385.
- [31]. Zhao Y, Jin J, Yang X, 2007. *Hydrothermal synthesis of titanate nanowire arrays*. *Materials Letters*, 61(2): 384-388.
- [32]. Yoo H, Kim M, Bae C, et al, 2014. *Understanding Photoluminescence of Monodispersed Crystalline Anatase TiO₂ Nanotube Arrays*. *The Journal of Physical Chemistry C*, 118(18): 9726-9732.
- [33]. Mercado C C, Knorr F J, McHale J L, et al, 2012. *Location of Hole and Electron Traps on Nanocrystalline Anatase TiO₂*. *The Journal of Physical Chemistry C*, 116(19): 10796-10804.
- [34]. Sikhvivilu L M, Mpelane S, Mwakikunga B W, et al, 2012. *Photoluminescence and Hydrogen Gas-Sensing Properties of Titanium Dioxide Nanostructures Synthesized by Hydrothermal Treatments*. *ACS Applied Materials & Interfaces*, 4(3): 1656-1665.
- [35]. Kongkanand A, Tvrdy K, Takechi K, et al, 2008. *Quantum Dot Solar Cells. Tuning Photoresponse through Size and Shape Control of CdSe-TiO₂ Architecture*. *Journal of the American Chemical Society*, 130(12): 4007-4015.